© The American Society of Gene & Cell Therapy

Minicircle DNA Vectors Achieve Sustained Expression Reflected by Active Chromatin and Transcriptional Level

Lia E. Gracey Maniar[1], Jay M. Maniar[1], Zhi-Ying Chen[2], Jiamiao Lu[2], Andrew Z. Fire[1,3] and Mark A. Kay[1,2]

[1]Department of Genetics, Stanford University School of Medicine, Stanford, California, USA; [2]Department of Pediatrics, Stanford University School of Medicine, Stanford, California, USA; [3]Department of Pathology, Stanford University School of Medicine, Stanford, California, USA

Current efforts in nonviral gene therapy are plagued by a pervasive difficulty in sustaining therapeutic levels of delivered transgenes. Minicircles (plasmid derivatives with the same expression cassette but lacking a bacterial backbone) show sustained expression and hold promise for therapeutic use where persistent transgene expression is required. To characterize the widely-observed silencing process affecting expression of foreign DNA in mammals, we used a system in which mouse liver presented with either plasmid or minicircle consistently silences plasmid but not minicircle expression. We found that preferential silencing of plasmid DNA occurs at a nuclear stage that precedes transport of mRNA to the cytoplasm, evident from a consistent >25-fold minicircle/plasmid transcript difference observed in both nuclear and total RNA. Among possible mechanisms of nuclear silencing, our data favor chromatin-linked transcriptional blockage rather than targeted degradation, aberrant processing, or compromised mRNA transport. In particular, we observe dramatic enrichment of H3K27 trimethylation on plasmid sequences. Also, it appears that Pol II can engage the modified plasmid chromatin, potentially in a manner that is not productive in the synthesis of high levels of new transcript. We outline a scenario in which sustained differences at the chromatin level cooperate to determine the activity of foreign DNA.

Received 16 April 2012; accepted 21 August 2012; advance online publication 27 November 2012. doi:10.1038/mt.2012.244

INTRODUCTION

Gene therapy is a promising treatment modality for single gene disorders, with several obstacles remaining before this technology can be used as a mainstay in the clinic.[1] In theory, nonviral DNA vectors provide a simple mode of gene transfer with potentially fewer side effects than other vehicles, such as viral vectors.[2] However, in mice, it has consistently been observed that exogenous transgenes in bacterial plasmid-based vectors are efficiently silenced in quiescent tissue such as the liver within the first several weeks after tail vein-mediated hydrodynamic transfection.[3–6]

The liver has been a particularly encouraging site for pilot gene therapies; transient curative levels of transgene expression have been achieved for a number of hepatodeficiency genetic diseases, including inborn errors of metabolism, hemophilia, and human alpha 1-antitrypsin (hAAT) deficiency.[7,8] hAAT is a liver-produced and secreted serine protease inhibitor (serpin) that inhibits the digestive activity of various proteinases. hAAT deficiency is relatively common (with a similar incidence as cystic fibrosis in Caucasian newborns) and often leads to early-onset chronic obstructive pulmonary disease due to unchecked digestion of the extracellular matrix in lung tissue as well as liver disease due to accumulation of nonsecreted AAT in hepatocytes.[9] Approximately 2% of children with a liver phenotype go on to develop fulminant liver disease and require liver transplantation.[10] Although normal circulating levels of hAAT are 2 mg/ml, only 20% of this level is projected to be necessary for symptom alleviation.[9] Several trials have been conducted in replacing hAAT using various viral vectors, but all have had difficulty in achieving therapeutic doses.[7,11,12]

Minicircles, which are derived from a parent plasmid by removing the bacterial backbone,[13] have been a promising DNA vehicle for gene replacement. Minicircles contain a minimal expression cassette, consisting of a promoter, transgene, and polyadenylation signal but are devoid of bacterial plasmid DNA elements.[13] It has been shown that minicircles are capable of sustaining expression for months at levels that are eventually 10 to 1000-fold higher than their plasmid counterparts.[13–15] Previously, the production of large amounts of minicircle DNA was highly time and labor intensive in comparison with making plasmid DNA given that minicircles do not contain bacterial elements such as selectable markers and origins of replication. Recently, significant improvements have been made in the production of minicircles, which now requires a similar amount of time, labor, and cost as plasmid production.[16] Although predominantly studied in the liver, minicircles have been used to achieve therapeutic levels of gene transfer in multiple tissue types, including heart and skeletal muscle.[17] In addition to their prospect as a gene therapy vehicle, minicircles have also shown promise in engineering manipulations used for generating pluripotent stem cells.[18]

Despite the potential significance for future applications, we have a poor fundamental understanding of the mechanism responsible for the expression difference between minicircles and plasmids. The ability to maintain concentrations of plasmid and minicircle DNA are not different *in vivo*, thus a mere loss of DNA is not responsible for the differential silencing that is observed.[13] Likewise, in the absence of a lipid carrier, methylation of CpG

Correspondence: *Mark A. Kay, 269 Campus Drive, CCSR Building, Room 2105, Stanford, CA 94305-5164, USA. E-mail: markay@stanford.edu*

© The American Society of Gene & Cell Therapy

motifs does not appear to be responsible for the expression difference. CpG-less plasmids only have a modest difference in expression for multiple transgenes, and varying the methylation status in minicircles does not affect long term transgene expression *in vivo*.[19] At some level, sequence differences between plasmid and minicircle are likely responsible for the expression differences. Given that the differences in expression have been implicitly tied to post-DNA events, there are many levels where regulatory differences might occur: transcription, pre-mRNA processing, degradation and/or nuclear transport, mRNA stability and translation. Currently, there is little support to include or exclude any of these mechanisms.

Work towards understanding the differences between silenced and active transgenes in direct DNA delivery has proceeded along several parallel lines. In efforts toward building better expression vectors, a series of different sequence elements have been added and removed, with analysis of the resulting transgenics for protein or RNA endpoints of expression.[2] These studies are of great value, but they do not resolve the mechanistic source of silencing. Our group has begun to investigate the properties of chromatin on minicircles and plasmids. Episomal DNA constructs with persistent expression have been found to have a modestly greater abundance (by 1.7-fold) of histone H3 lysine 4 di-methylation (H3K4me2), while unexpressed constructs showed enrichment (by 1.5-fold) in histone H3 lysine 9 trimethylation (H3K9me3).[20] Although of considerable interest, it is unclear how such modest bulk differences alone would mechanistically explain the substantial differences in activity. This leaves open many questions, including at which level silencing is enforced and what molecular characteristics maintain a distinction between silenced and active transgenes.

RESULTS

To study *in vivo* expression, we used a plasmid with a Rous sarcoma virus promoter driving a hAAT cDNA transgene (**Figure 1a**). From this parent plasmid, we derived a minicircle that contained an identical expression cassette lacking the bacterial DNA elements (**Figure 1b**).[13] Plasmid or minicircle DNA was then delivered to 6 to 8-week-old C57/Bl6 female mice by hydrodynamic tail vein injection. Following this type of injection, naked vector DNA is preferentially taken up by hepatocytes,[3,21] with the injected DNA persisting in an episomal state. Livers were harvested at 6 weeks post-infusion. Copy numbers per cell were comparable between plasmid and minicircle injections (1.8 copies for the plasmid injections and 1.5 copies for the minicircle injections) in the harvested livers.

We measured transgene expression using multiple methods. To follow protein production, we quantified serum levels of hAAT over time by enzyme-linked immunosorbent assay. At 3 days post-injection, high and similar levels of hAAT were produced in both plasmid and minicircle-injected mice (**Figure 1c**). As expected, by 6 weeks the plasmid expression was effectively silenced and the minicircle-injected mice produced 30–40 times more hAAT protein than plasmid-injected mice (**Figure 1c**). For the described experiments, we harvested the transfected livers at 6 weeks post-injection, when DNA was stable in the nucleus and we observed a difference in transgene expression. At this timepoint, minicircle was still expressing while plasmid-mediated expression had been silenced.

Expression differentials at the level of RNA accumulation

To evaluate the silencing process at an RNA level, we carried out both northern blotting and RNA-Seq for liver RNA from mice injected with plasmid or minicircle. Northern blotting of samples at day 1 and day 140 (with similar expression levels as week 6) after injection suggested a difference in mature mRNA (**Supplementary Figure S1** online). We then proceeded with RNA-Seq as a means to both quantitate this difference and to look for additional RNAs that may be present during silencing.

Our analyses showed abundant levels of transgene-derived tags from the sense strand in minicircle-injected liver, with only sparse occurrence of such tags from the plasmid-injected liver (**Figure 2**; biological replicates in **Supplementary Figure S2** online). We calculated values of 45.3–51.7 reads per kilobase of exon per million reads (RPKM)[22] for hAAT transcript from minicircle and 1.6–1.8 RPKM for transcript from plasmid (**Table 1**). For mouse liver, it had previously been found that a value of 3 RPKM corresponded to ~1 transcript per liver cell.[22] In our dataset, other genomic transcripts with similar RPKM values to minicircle included widely expressed housekeeping genes and liver-specific genes. Endogenous transcript RPKM

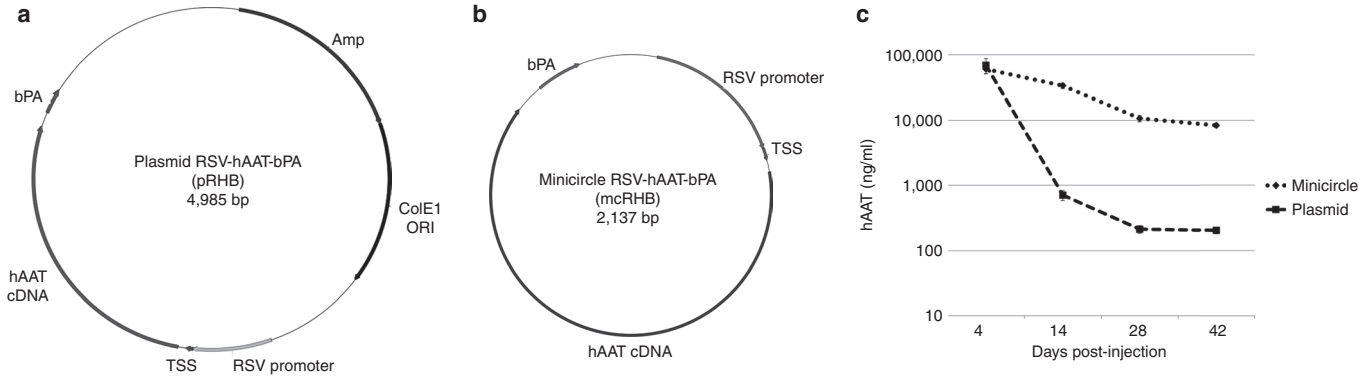

Figure 1 Vector maps and protein expression levels of plasmid and minicircle carrying the human alpha-1 antitrypsin (hAAT) expression cassette. (**a**) Plasmid. (**b**) Minicircle. (**c**) Enzyme-linked immunosorbent assay data following the production of secreted hAAT protein in circulating blood over time. Error bars represent standard error. At least five mice were injected in each DNA group. Amp, Ampicillin resistance marker; bPA, bovine poly-A signal; ColE ORI, *Escherichia coli* origin of replication; RSV, Rous sarcoma virus promoter; TSS, transcription start site.

© The American Society of Gene & Cell Therapy

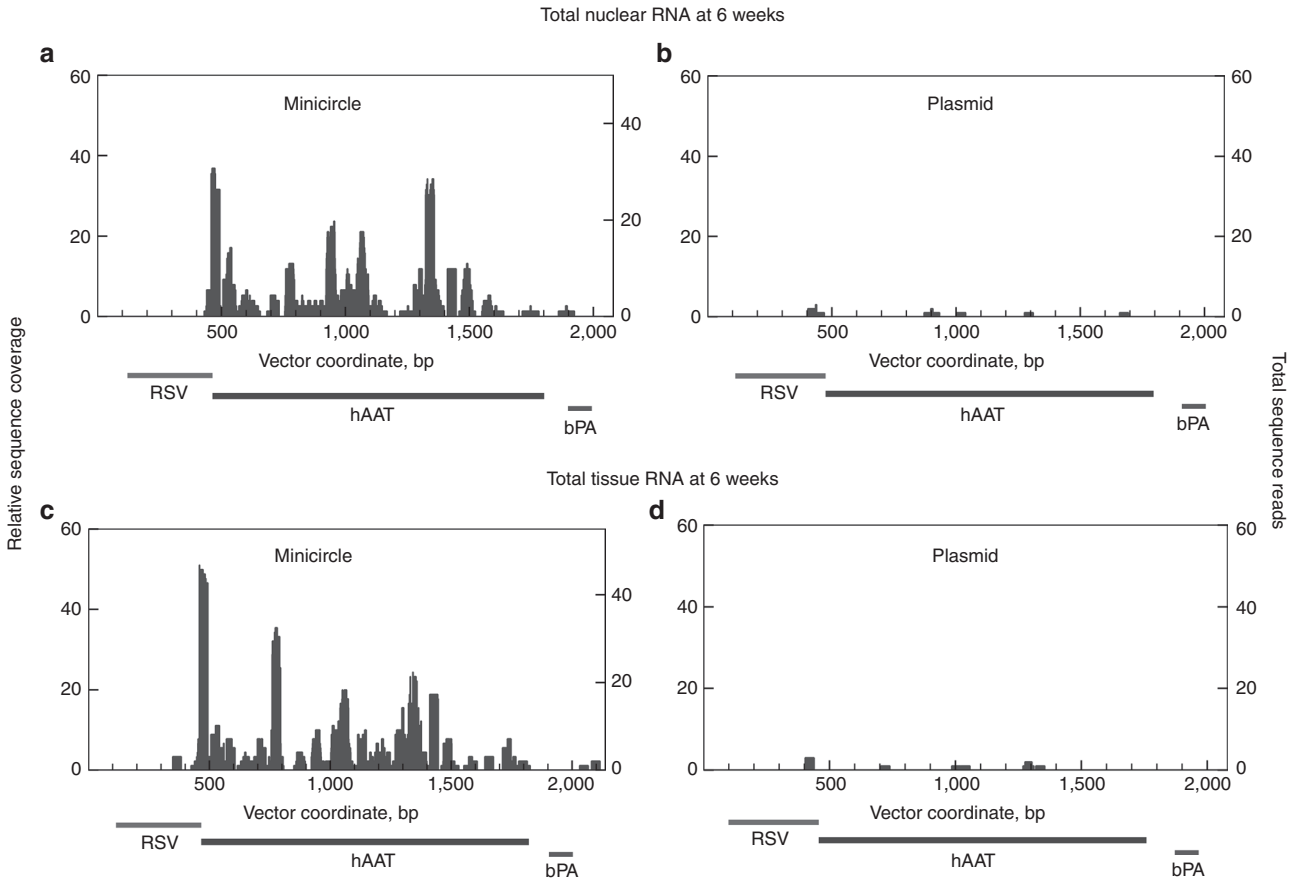

Figure 2 Total tissue and nuclear RNA coverage of the sense strand of minicircle or plasmid from RNA-Seq of mouse livers harvested at 6 weeks post-injection. (**a**) Coverage of minicircle from total nuclear RNA. (**b**) Coverage of plasmid from total nuclear RNA. (**c**) Coverage of minicircle from total tissue RNA. (**d**) Coverage of plasmid from total tissue RNA.

Table 1 RPKM values from RNA-Seq for plasmid and minicircle in mouse liver at 6 weeks post-injection

Plasmid	Minicircle
Total RNA	Total RNA
1.6 RPKM	45.3 RPKM
Nuclear RNA	Nuclear RNA
1.8 RPKM	51.7 RPKM

RPKM, reads per kilobase of exon per million reads.

levels similar to plasmid were largely annotated as hypothetical transcripts, tissue specific (non-liver) genes, and developmentally regulated genes that are expressed during various stages of embryogenesis.

The presence of reads derived from the plasmid suggested either a very low level of transcription occurring from selected copies of the plasmids (consistent with residual levels of protein observed from plasmid injectees at 6 weeks, **Figure 1b**) and/or aberrant transcription. Although transcription from the plasmid was rare, transcripts appeared to be properly initiated; 5′ RACE results from plasmid at 6 weeks post-injection indicated the generation of at least some transcripts to enable the capture of proper 5′ ends identical to those derived from minicircle (**Supplementary Figure S3** online).

Strand-specificity appeared to be maintained for both transgene modalities, with very little (if any) transcript from the antisense strand of the minicircle or from either strand of the plasmid (**Figure 2** and **Supplementary Figure S4** online). This argues against an antisense-mediated mechanism in silencing of plasmid expression.

To further pinpoint where the silencing process occurred, we next analyzed RNA patterns for RNA from whole liver and from isolated nuclei.[23] To assess the quality of nuclear isolation, we examined the sequences for the enrichment of known nuclear RNAs. These analyses confirmed a substantial 10 to 20-fold enrichment for known nuclear RNAs (**Supplementary Table S1** online). Overall patterns of read coverage were very similar in both total tissue RNA and nuclear-only RNA (**Figure 2**), but again with significantly higher levels of minicircle than plasmid RNA. The coverage in the nuclear samples was comparable to that observed with total tissue RNA, arguing for a nuclear origin in the differential expression of plasmid and minicircle DNA.

MNase-Seq and ChIP-Seq-based analyses of chromatin features associated with minicircle and plasmid transgenes

We performed micrococcal nuclease digestion followed by high-throughput sequencing (MNase-Seq) and chromatin immunoprecipitation followed by sequencing (ChIP-Seq) to study the

© The American Society of Gene & Cell Therapy

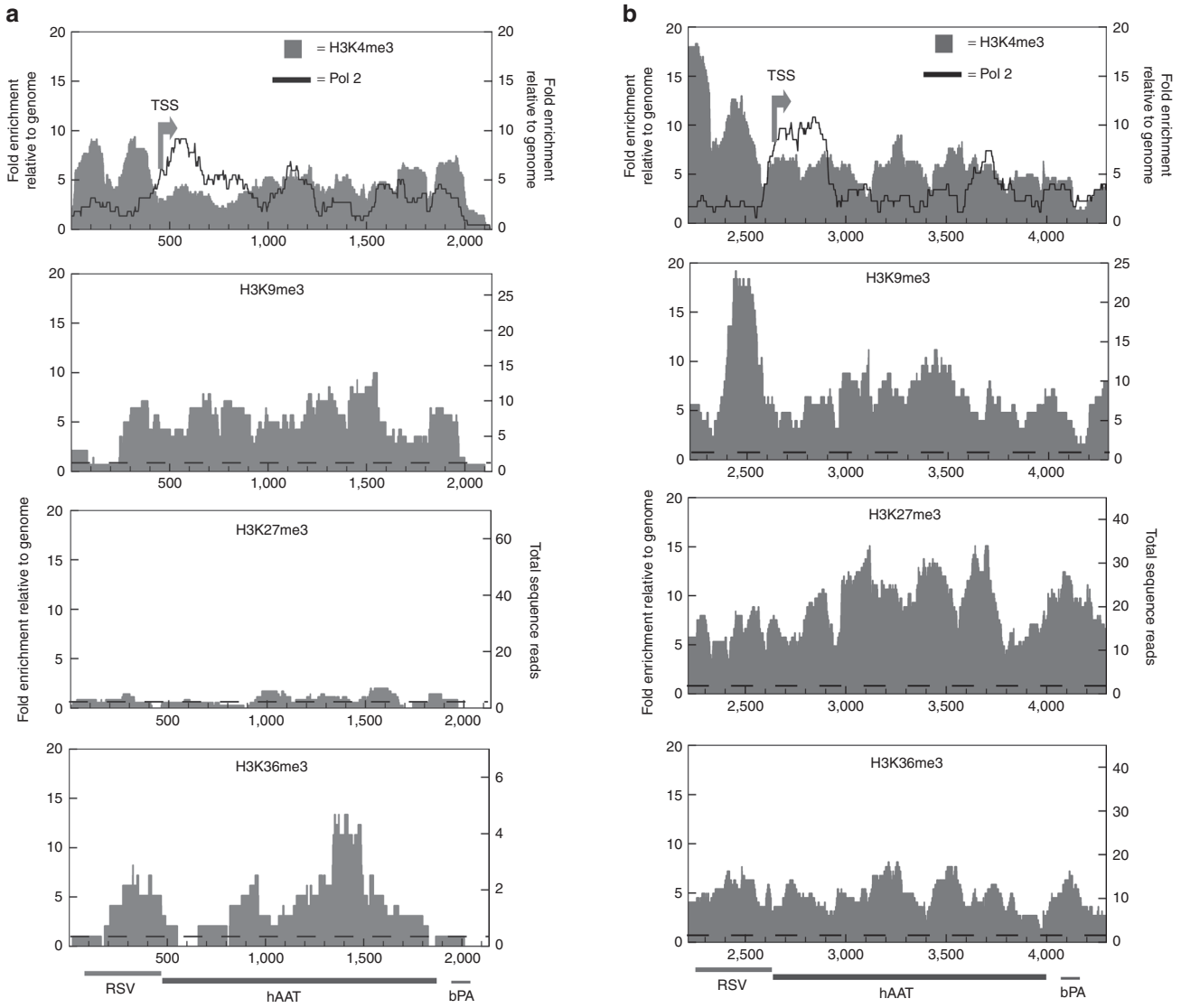

Figure 3 Coverage of histone modifications and RNA polymerase II on plasmid and minicircle from ChIP-Seq of mouse liver at 6 weeks post-injection. Dashed line is at $y = 1$, where enrichment is equal to the average signal seen in the genome at random. (**a**) Minicircle coverage. (**b**) Plasmid coverage.

chromatin structure of minicircle and plasmid at a high resolution at a 6-week post-injection timepoint. We performed at least two biological replicates for each sample (**Supplementary Figure S5** online) and input controls (**Supplementary Figure S6c,d** online). MNase-Seq provided an overall nucleosome positioning map (**Supplementary Figure S6a,b** online), with no selection for any specific type of nucleosome, while ChIP allowed stratification of the resulting map into different histone modification subsets. Because the sequencing assays were genome-wide, we were able to confirm the specificity and quality of the assays by examining patterns of nucleosome positioning, histone modifications, and RNA polymerase II occupancy at numerous well-characterized genomic loci (**Supplementary Figure S7** online).

Nucleosome positioning. In bulk populations of nucleosomes from plasmid and minicircle livers, we observed nucleosomes throughout each construct with varying degrees of coverage over the entire transgene. In both cases, we observed a well-defined structure with positioned nucleosomes around the promoter, but with more apparent phasing, or regular organization of nucleosomes, throughout the minicircle cDNA and not on the plasmid (**Supplementary Figure S6** online). In some model systems, a nucleosome-free region is found at expressed genes upstream of the transcription start site (TSS), although less frequently in mammals than in yeast.[24] No strong nucleosome-free region region was evident for either plasmid or minicircle.

RNA polymerase II. RNA polymerase (Pol II) is enriched at actively expressed genes, but is also found at the promoters of unexpressed genes in a "poised" state without active elongation.[25,26] We observed a prominent peak of Pol II signal at the TSS of the plasmid (**Figure 3b**) and a smaller peak at the 3′ end of the cDNA, but saw very little Pol II elsewhere in the vector (**Supplementary Figure S8** online). In contrast, we observed peaks of Pol II

© The American Society of Gene & Cell Therapy

throughout the minicircle expression cassette (proximal promoter + hAAT cDNA) (**Figure 3a**).

H3K4me3. Histone H3 lysine 4 trimethylation (H3K4me3) has been well-established as a general marker of expressed genes in many studied genomes.[27] H3K4me3 is also thought to be a remnant marker on genes that were expressed at earlier developmental stages, even if they are no longer actively transcribed.[28]

In both minicircle and plasmid, we saw distinct peaks of H3K4me3 enrichment, but in different patterns (**Figure 3**). In the minicircle, there were two well-positioned nucleosomes with H3K4me3 upstream of the TSS and two well-positioned nucleosomes at the 3′ poly-A signal (**Figure 3a**). This configuration exhibits considerable similarity to nucleosome patterns that have been described for a number of expressed endogenous genes, where well-positioned nucleosomes at the TSS are frequently followed by nucleosomes with more flexible positioning with increasing distance downstream from the TSS, and an additional region of strong positioning at the 3′ end.[29,30] The plasmid also showed peaks of H3K4me3, but with local differences as compared with minicircle and less well-defined patterning at the 3′ end of the cDNA (**Figure 3b**).

H3K9me3. Histone H3 lysine 9 trimethylation (H3K9me3) is known to be enriched at a set of silenced regions in the genome, including at repetitive regions and nonexpressed genes; still, some H3K9me3 is also present on active genes.[31,32] We found ~1.5 to 2-fold higher levels of H3K9me3 on the plasmid versus the minicircle throughout the expression cassette (**Figure 3**). Much of the differential signal appeared concentrated at a single peak just upstream of the TSS, the plasmid.

H3K27me3. Histone H3 lysine 27 trimethylation (H3K27me3) has been found at silenced genes that were initially expressed at a specific developmental timepoint.[27] The largest overall difference in transgene modification between minicircle and plasmid that we observed was in H3K27me3 levels (**Figure 3**). We observed a 5 to 15-fold enrichment over the expression cassette of the plasmid (**Figure 3b**) and an abundance of signal over the bacterial backbone (**Supplementary Figure 8** online). Significantly, we did not see an enrichment of this silencing mark on the minicircle (**Figure 3a**).

H3K36me3. Histone H3 lysine 36 trimethylation (H3K36me3) enrichment, especially toward the 3′ end of a gene, is often a characteristic property for a subset of expressed genes.[27] In addition to expressed loci showing enrichment for H3K36 methylation, recent reports describe a type of euchromatin that is characterized by a lack of prominent H3K36me3 peaks[33] and a dependence on intron content and splicing for H3K36me3 enrichment.[34,35] In the H3K36me3-enriched nucleosome libraries derived for this work, we saw examples of expressed endogenous mouse genes with and without H3K36me3 enrichment (**Supplementary Figure S7d** online).

We saw a relatively modest enrichment of H3K36me3 signal on minicircle DNA, but with a >10-fold enrichment of H3K36me3 at the 3′ end of the cDNA gene (**Figure 3a**), consistent with the characteristic pattern observed in some well-expressed genes. Intriguingly, a fivefold enrichment of this modification was observed over the expression cassette on the plasmid vector (**Figure 3b**).

DISCUSSION

Mechanisms leading to silencing of foreign DNA, readily observed in many biological systems, have led to both challenges and opportunities in understanding gene expression and in applications of engineered gene expression.[1,36–40] Silencing processes in well-studied models include mechanisms regulating DNA integrity, DNA methylation, accessibility and transcription of chromatin, and stability of cytoplasmic RNA.

Our high-resolution analysis of chromatin provided both general properties and detailed maps of the plasmid and minicircle chromatin. We were particularly interested in the striking enrichment of H3K27me3 on the plasmid as compared with the minicircle at a timepoint when expression from the plasmid was silenced and the minicircle was still expressing. We also observed a modest enrichment of plasmid with H3K9me3, similar to the 1.5-fold enrichment that was previously found on comparable expression cassettes.[20] This is consistent with some relationship between this chromatin mark and the events marking the silenced locus, but substantially smaller in magnitude than the observed H3K27me3 presence. Therefore, an enrichment of H3K27me3 could be an important mark that distinguishes a silent episome from an active one, suggesting a role of the polycomb-group proteins in the regulation of plasmid DNA expression.[27]

Modification of histone H3 by methylation at K4 and K36 are both associated with actively transcribed regions, with their distributions likely demarcating different characteristics of active chromatin. Similar distinctions have been reported in analyses of H3K36 methylation in diverse cell systems, with some correlation to the intron content of genes[34,35] and to expression.[41] In the plasmid and minicircle constructs used here, the expression cassette was derived from cDNA, thereby lacking introns. We saw relatively sparse coverage of H3K36me3 on the minicircle, but the localized enrichment occurred at the 3' end of the gene, which is a characteristic area of enrichment for many expressed endogenous genes.[42] The K4me3 and K36me3 marks that we observed with plasmid several weeks after injection were associated with little transcript production. In this case, these modifications could reflect previous transcriptional events. We also may have enriched for the few copies of plasmid that were still active at a basal level in the liver as evidenced from positive 5′ RACE results (**Supplementary Figure S3** online) and the presence of low levels of RNA-Seq tags from plasmid. In addition, the plasmid expression cassette may have a bivalent chromatin structure. In stem cells, bivalent domains at certain developmentally regulated genes have both H3K4me3 and H3K27me3 enrichment, marking them as silent but poised for activation.[43]

The pattern of Pol II coverage on the plasmid and minicircle fits with patterns that have previously been observed genome-wide. Pol II at the minicircle was present throughout the expression cassette, suggesting the presence of active transcription. However, in the plasmid, Pol II was concentrated at the promoter, as has been observed at inactive genes in metazoan genomes.[26]

Overall, we observed histone marks consistent with silenced and expressed genes on both the plasmid and minicircle. Since

© The American Society of Gene & Cell Therapy

we were studying a temporal snapshot of cells from the liver, each sample would be expected to consist of a population of cells including both expressed and nonexpressed transgene copies. The observed Pol II and histone modification properties were reflective of specific aspects of patterns previously observed on a genome-wide basis at endogenous loci,[27,42] though unique aspects were also evident.

Chromatin structure in *Saccharomyces cerevisiae* has been extensively studied as a function of promoter type, histone modifications, and expression characteristics.[44] In comparing the regulation of minicircle and plasmid with well-characterized yeast promoters, the chromatin structure of our constructs was most consistent with that of TATA-box containing promoters in yeast. TATA-containing yeast promoters tend to lack a prominent nucleosome-free region, with the TATA element often obscured by a nucleosome.[45] The Rous sarcoma virus promoter in our expression cassette lacked poly dA/dT elements, contained a TATA-box, and had the TATA sequence wrapped up in a nucleosome.

Yeast genes whose promoters contain a TATA-box are thought to be environmentally responsive, while promoters that lack a TATA-box are more frequently observed to have a canonical promoter structure with a nucleosome-free region upstream of the TSS and are associated with housekeeping genes.[44] In recent work, it was proposed that promoters in yeast with high occupancy of nucleosomes within 150 bp of the TSS and dynamic nucleosome positioning in the rest of the vicinity were found to have large transcriptional changes in response to environmental stimuli.[46] These properties argue for an analogy between active exogenous constructs in mouse liver and a set of environmentally regulated yeast promoters. In support of the significance of promoters primed to respond to the environment, it has been shown that silenced plasmids in the mouse liver could be reactivated by repeated hydrodynamic delivery of saline.[47,48] Hydrodynamic injection is known to be a physiologically demanding procedure, with increased oxidative stress and interleukin production,[48] as well as increased activity of transcription factors activator protein-1 and nuclear factor-kappa B.[47]

The importance in understanding the mechanism of transgene silencing is critical to the development of improved gene transfer vectors for the treatment of many significant diseases. Uncovering these fundamental properties will be important to our understanding of how genes are regulated as well as attaining the most robust approaches for achieving high-level exogenous transgene expression, useful both in biological discovery and gene therapeutics**.**

METHODS

Animal studies. All animal procedures were conducted in accordance with guidelines set by the National Institutes of Health, the Animal Welfare Act, and the Stanford University School of Medicine. All procedures were approved by the Institutional Animal Care and Use Committee.

C57/Bl6 female mice at 6–8 weeks of age were used for all experiments. Using a hydrodynamic (high-volume) injection protocol,[3,21] 20 ug of plasmid DNA in 0.9% saline were injected into the tail vein of the mice. DNA was prepared as previously described[13,15] and checked for integrity by agarose gel electrophoresis. Serum samples were collected at several time points after injection via retro-orbital bleeding for hAAT protein quantification by enzyme-linked immunosorbent assay. Biological replicates were obtained by harvesting livers from different injected animals.

Chromatin immunoprecipitation. Chromatin was isolated by grinding frozen mouse liver tissue in liquid nitrogen and briefly crosslinking material in 1% formaldehyde in buffer A (15 mmol/l HEPES–Na (pH 7.5), 60 mmol/l KCl, 15 mmol/l NaCl, 0.15 mmol/l β-mercaptoethanol, 0.15 mmol/l spermine, 0.15 mmol/l spermidine, 0.34 mol/l sucrose), 0.5 mmol/l phenylmethanesulfonyl fluoride, 1/100 dilution of protease inhibitor set III (Cal Biochem, Darmstadt, Germany), and 1 mmol/l dithiothreitol, for 20 minutes at room temperature. Crosslinking was quenched with glycine to 125 mmol/l. $CaCl_2$ was added to 2 mmol/l and micrococcal nuclease (MNase; Roche, Indianapolis, IN)) was titrated to digest the majority of chromatin to mononucleosomes at 37 °C, as described.[49] EGTA was added to a concentration of 10 mmol/l to stop the reaction.

The reaction was briefly spun and the pellet with insoluble chromatin was resuspended in RIPA buffer (1× phosphate-buffered saline, 1% NP-40, 0.5% sodium deoxycholate, 0.1% sodium dodecyl sulfate, 1× HALT protease and phosphatase inhibitor, 1 mmol/l phenylmethanesulfonyl fluoride) and 2 mmol/l EGTA. Chromatin was solubilized by sonication with a Microson TM XL 2000 (microtip probe; Qsonica, Newtown, CA) five times for 30 seconds each at level 5, with 1 minute on ice in between each sonication. A 1/10 volume of 10% Triton-X was added to the lysate. The lysate was spun at full speed at 4 °C for 5 minutes and the supernatant containing soluble chromatin was collected. Input chromatin was precleared with Dynal beads conjugated with protein A (Invitrogen, Grand Island, NY) that had been washed three times with 1× phosphate-buffered saline plus 0.5% bovine serum albumin.

Each immunoprecipitation reaction was carried out as described, with minor modifications.[49,50] Antibodies used in this work had previously been shown to perform well in ChIP experiments (see **Supplementary Materials and Methods** online). Briefly, 5 µg antibody was coupled to Dynal beads conjugated with protein A (Invitrogen). Precleared input chromatin was added to the beads and the reaction was incubated overnight at 4 °C. The beads were washed four times with lithium chloride wash buffer (100 mmol/l Tris-HCl, pH 7.5, 500 mmol/l LiCl, 1% NP-40, 1% sodium deoxycholate), followed by one wash with TE + 50 mmol/l NaCl. Immunoprecipitated material was eluted and crosslinks were reversed by adding 400 ul of lysis buffer (0.1 mol/l Tris-HCl, pH 7.5, 0.1 mol/l NaCl, 1% sodium dodecyl sulfate, 50 mmol/l ethylenediaminetetraacetic acid) with 0.2 mg/ml proteinase K and incubating for 6 hours at 65 °C, with frequent vortexing. DNA was recovered after organic extraction and ethanol precipitation. Adapters were ligated to the ends of the DNA and the fragments were minimally PCR-amplified to isolate an unsaturated reaction to avoid bottlenecking and reannealing bias. Libraries were sequenced using either the Illumina GAIIx or HiSeq platforms (Illumina, San Diego, CA).

RNA extraction and assays. Nuclei were collected from frozen mouse liver grinds using the Nuclei PURE Prep isolation (Sigma, St Louis, MO). In brief, lysed cells were spun through a stringent 2 mol/l sucrose cushion and nuclei were pelleted by ultracentrifugation at 30000*g* for 45 minutes at 4 °C. Nuclear and total tissue RNA was isolated using the early steps of the miRvana miRNA Isolation kit (Ambion, Grand Island, NY). Total RNA was either Poly-A selected using the Poly(A)Purist mRNA isolation kit (Ambion) or de-enriched for rRNA using the Ribominus Eukaryote kit for RNA-Seq (Invitrogen). RNA was treated with DNAse to remove any contaminating genomic DNA, followed by organic extraction and ethanol precipitation. Directional RNA-Seq libraries were built using the ScriptSeq mRNA-Seq library preparation kit (Illumina-compatible, Epicentre) and sequenced using the Illumina GAIIx platform.

To capture 5′ ends of transcripts, 5′ RACE was carried out on poly-A selected RNA using the First Choice RLM-Race method (Ambion). Negative control samples were produced by omitting reverse transcriptase from RNA samples.

© The American Society of Gene & Cell Therapy

For northern blotting, animals were sacrificed on day 1 and day 140 after injection. Total RNA was extracted from mouse liver and run on 1% denaturing agarose gel. The northern blot was probed with a 220 bp P32-labeled hAAT cDNA probe to detect hAAT mRNA. The probe was generated via PCR by using primers 5′GCCGTCTTCTGTCTCGTGG3′ and 5′AAGAAGATATTGGTGCTGTTGG3 ′. After stripping, the same northern blot was re-probed with P32-labeled β-actin probe to detect β-actin as a loading control.

Selective hybridization. Selective hybridization of bulk nucleosomes was carried out as previously described.[6] In brief, a biotin-labeled probe against a 1.5 kb portion of the vector was generated using a biotin-labeled PCR primer and made single-stranded by stripping away the second strand with 125 mmol/l NaOH. The single-stranded probe was bound to streptavidin-coated Dynabeads (Invitrogen) and mixed with amplified Illumina-linkered nucleosome core DNA populations from mouse liver in hybridization buffer (12X SSC, 2X Denhardt's solution) with an equal volume of formamide. After washing and boiling, the hybridized DNA was PCR-amplified for a minimal number of rounds and sequenced using the Illumina GAIIx platform.

SUPPLEMENTARY MATERIAL

Figure S1. Northern blotting with total liver RNA to evaluate hAAT RNA production from plasmid and minicircle at early and late post-injection timepoints.

Figure S2. Dot plots comparing read alignment counts from biological replicates of RNA-Seq samples from nuclear and total tissue RNA.

Figure S3. 5′RACE to capture 5′ ends of transcripts produced from plasmid or minicircle.

Figure S4. Total tissue and nuclear RNA coverage of the antisense strand of plasmid and minicircle from mouse livers harvested at 6 weeks post-injection.

Figure S5. Dot plots comparing read alignment counts from biological replicates of ChIP-Seq samples.Figure S6. Selective hybridization of mouse livers injected with either minicircle (A) or plasmid (B) DNA displays overall nucleosome patterns.

Figure S7. Evaluation of ChIP-Seq enrichments at genomic loci representing regions with expression and lack of expression.

Figure S8. Bacterial backbone ChIP-Seq enrichments along the entire plasmid sequence.

Table S1. Evaluation of nuclear RNA fractionation.

Materials and Methods.

ACKNOWLEDGMENTS

We thank Sam Gu, Ayelet Lamm, Qingjun Luo,Yue Zhang, Zimeng Weng, Phil Lacroute, Arend Sidow, Feijie Zhang, and Cheng-Yi He for their help and guidance during this work. L.G.M. is supported by the National Institutes of Health under Ruth L. Kirschstein National Research Service Award 5F30HL09639603. M.A.K. is supported by R01 HL064274.

REFERENCES

1. Kay, MA (2011). State-of-the-art gene-based therapies: the road ahead. *Nat Rev Genet* **12**: 316–328.
2. Glover, DJ, Lipps, HJ and Jans, DA (2005). Towards safe, non-viral therapeutic gene expression in humans. *Nat Rev Genet* **6**: 299–310.
3. Zhang, G, Budker, V and Wolff, JA (1999). High levels of foreign gene expression in hepatocytes after tail vein injections of naked plasmid DNA. *Hum Gene Ther* **10**: 1735–1737.
4. Yant, SR, Meuse, L, Chiu, W, Ivics, Z, Izsvak, Z and Kay, MA (2000). Somatic integration and long-term transgene expression in normal and haemophilic mice using a DNA transposon system. *Nat Genet* **25**: 35–41.
5. Gill, DR, Pringle, IA and Hyde, SC (2009). Progress and prospects: the design and production of plasmid vectors. *Gene Ther* **16**: 165–171.
6. Gracey, LE, Chen, ZY, Maniar, JM, Valouev, A, Sidow, A, Kay, MA *et al.* (2010). An *in vitro*-identified high-affinity nucleosome-positioning signal is capable of transiently positioning a nucleosome in vivo. *Epigenetics Chromatin* **3**: 13.
7. Stecenko, AA and Brigham, KL (2003). Gene therapy progress and prospects: alpha-1 antitrypsin. *Gene Ther* **10**: 95–99.
8. High, KA (2011). Gene therapy for haemophilia: a long and winding road. *J Thromb Haemost* **9 Suppl 1**: 2–11.
9. Kay, MA, Graham, F, Leland, F and Woo, SL (1995). Therapeutic serum concentrations of human alpha-1-antitrypsin after adenoviral-mediated gene transfer into mouse hepatocytes. *Hepatology* **21**: 815–819.
10. Silverman, EK and Sandhaus, RA (2009). Clinical practice. Alpha1-antitrypsin deficiency. *N Engl J Med* **360**: 2749–2757.
11. Flotte, TR, Trapnell, BC, Humphries, M, Carey, B, Calcedo, R, Rouhani, F *et al.* (2011). Phase 2 clinical trial of a recombinant adeno-associated viral vector expressing a1-antitrypsin: interim results. *Hum Gene Ther* **22**: 1239–1247.
12. Osborn, MJ, McElmurry, RT, Lees, CJ, DeFeo, AP, Chen, ZY, Kay, MA *et al.* (2011). Minicircle DNA-based gene therapy coupled with immune modulation permits long-term expression of a-L-iduronidase in mice with mucopolysaccharidosis type I. *Mol Ther* **19**: 450–460.
13. Chen, ZY, He, CY, Ehrhardt, A and Kay, MA (2003). Minicircle DNA vectors devoid of bacterial DNA result in persistent and high-level transgene expression in vivo. *Mol Ther* **8**: 495–500.
14. Chen, ZY, He, CY, Meuse, L and Kay, MA (2004). Silencing of episomal transgene expression by plasmid bacterial DNA elements in vivo. *Gene Ther* **11**: 856–864.
15. Chen, ZY, Yant, SR, He, CY, Meuse, L, Shen, S and Kay, MA (2001). Linear DNAs concatemerize *in vivo* and result in sustained transgene expression in mouse liver. *Mol Ther* **3**: 403–410.
16. Kay, MA, He, CY and Chen, ZY (2010). A robust system for production of minicircle DNA vectors. *Nat Biotechnol* **28**: 1287–1289.
17. Stenler, S, Andersson, A, Simonson, OE, Lundin, KE, Chen, ZY, Kay, MA *et al.* (2009). Gene transfer to mouse heart and skeletal muscles using a minicircle expressing human vascular endothelial growth factor. *J Cardiovasc Pharmacol* **53**: 18–23.
18. Narsinh, KH, Jia, F, Robbins, RC, Kay, MA, Longaker, MT and Wu, JC (2011). Generation of adult human induced pluripotent stem cells using nonviral minicircle DNA vectors. *Nat Protoc* **6**: 78–88.
19. Chen, ZY, Riu, E, He, CY, Xu, H and Kay, MA (2008). Silencing of episomal transgene expression in liver by plasmid bacterial backbone DNA is independent of CpG methylation. *Mol Ther* **16**: 548–556.
20. Riu, E, Chen, ZY, Xu, H, He, CY and Kay, MA (2007). Histone modifications are associated with the persistence or silencing of vector-mediated transgene expression in vivo. *Mol Ther* **15**: 1348–1355.
21. Liu, F, Song, Y and Liu, D (1999). Hydrodynamics-based transfection in animals by systemic administration of plasmid DNA. *Gene Ther* **6**: 1258–1266.
22. Mortazavi, A, Williams, BA, McCue, K, Schaeffer, L and Wold, B (2008). Mapping and quantifying mammalian transcriptomes by RNA-Seq. *Nat Methods* **5**: 621–628.
23. Chauveau, J, Moule, Y and Rouiller, C (1956). Isolation of pure and unaltered liver nuclei morphology and biochemical composition. *Exp Cell Res* **11**: 317–321.
24. Rando, OJ and Chang, HY (2009). Genome-wide views of chromatin structure. *Annu Rev Biochem* **78**: 245–271.
25. Guenther, MG, Levine, SS, Boyer, LA, Jaenisch, R and Young, RA (2007). A chromatin landmark and transcription initiation at most promoters in human cells. *Cell* **130**: 77–88.
26. Zhou, Q, Li, T and Price, DH (2012). RNA polymerase II elongation control. *Annu Rev Biochem* **81**: 119–143.
27. Shilatifard, A (2006). Chromatin modifications by methylation and ubiquitination: implications in the regulation of gene expression. *Annu Rev Biochem* **75**: 243–269.
28. Ng, HH, Robert, F, Young, RA and Struhl, K (2003). Targeted recruitment of Set1 histone methylase by elongating Pol II provides a localized mark and memory of recent transcriptional activity. *Mol Cell* **11**: 709–719.
29. Schones, DE, Cui, K, Cuddapah, S, Roh, TY, Barski, A, Wang, Z *et al.* (2008). Dynamic regulation of nucleosome positioning in the human genome. *Cell* **132**: 887–898.
30. Mavrich, TN, Ioshikhes, IP, Venters, BJ, Jiang, C, Tomsho, LP, Qi, J *et al.* (2008). A barrier nucleosome model for statistical positioning of nucleosomes throughout the yeast genome. *Genome Res* **18**: 1073–1083.
31. Rosenfeld, JA, Xuan, Z and DeSalle, R (2009). Investigating repetitively matching short sequencing reads: the enigmatic nature of H3K9me3. *Epigenetics* **4**: 476–486.
32. Vakoc, CR, Mandat, SA, Olenchock, BA and Blobel, GA (2005). Histone H3 lysine 9 methylation and HP1gamma are associated with transcription elongation through mammalian chromatin. *Mol Cell* **19**: 381–391.
33. Filion, GJ, van Bemmel, JG, Braunschweig, U, Talhout, W, Kind, J, Ward, LD *et al.* (2010). Systematic protein location mapping reveals five principal chromatin types in Drosophila cells. *Cell* **143**: 212–224.
34. Kim, S, Kim, H, Fong, N, Erickson, B and Bentley, DL (2011). Pre-mRNA splicing is a determinant of histone H3K36 methylation. *Proc Natl Acad Sci USA* **108**: 13564–13569.
35. de Almeida, SF, Grosso, AR, Koch, F, Fenouil, R, Carvalho, S, Andrade, J *et al.* (2011). Splicing enhances recruitment of methyltransferase HYPB/Setd2 and methylation of histone H3 Lys36. *Nat Struct Mol Biol* **18**: 977–983.
36. Selker, EU (1997). Epigenetic phenomena in filamentous fungi: useful paradigms or repeat-induced confusion? *Trends Genet* **13**: 296–301.
37. Arber, W (1974). DNA modification and restriction. *Prog Nucleic Acid Res Mol Biol* **14**: 1–37.
38. Beachy, RN (1997). Mechanisms and applications of pathogen-derived resistance in transgenic plants. *Curr Opin Biotechnol* **8**: 215–220.
39. Fire, A, Albertson, D, Harrison, SW and Moerman, DG (1991). Production of antisense RNA leads to effective and specific inhibition of gene expression in C. elegans muscle. *Development* **113**: 503–514.
40. Cameron, FH and Jennings, PA (1991). Inhibition of gene expression by a short sense fragment. *Nucleic Acids Res* **19**: 469–475.
41. Morris, SA, Rao, B, Garcia, BA, Hake, SB, Diaz, RL, Shabanowitz, J *et al.* (2007). Identification of histone H3 lysine 36 acetylation as a highly conserved histone modification. *J Biol Chem* **282**: 7632–7640.

© The American Society of Gene & Cell Therapy

42. Barski, A, Cuddapah, S, Cui, K, Roh, TY, Schones, DE, Wang, Z *et al.* (2007). High-resolution profiling of histone methylations in the human genome. *Cell* **129**: 823–837.
43. Bernstein, BE, Mikkelsen, TS, Xie, X, Kamal, M, Huebert, DJ, Cuff, J *et al.* (2006). A bivalent chromatin structure marks key developmental genes in embryonic stem cells. *Cell* **125**: 315–326.
44. Jansen, A and Verstrepen, KJ (2011). Nucleosome positioning in Saccharomyces cerevisiae. *Microbiol Mol Biol Rev* **75**: 301–320.
45. Ioshikhes, IP, Albert, I, Zanton, SJ and Pugh, BF (2006). Nucleosome positions predicted through comparative genomics. *Nat Genet* **38**: 1210–1215.
46. Tirosh, I and Barkai, N (2008). Two strategies for gene regulation by promoter nucleosomes. *Genome Res* **18**: 1084–1091.
47. Nishikawa, M, Nakayama, A, Takahashi, Y, Fukuhara, Y and Takakura, Y (2008). Reactivation of silenced transgene expression in mouse liver by rapid, large-volume injection of isotonic solution. *Hum Gene Ther* **19**: 1009–1020.
48. Takiguchi, N, Takahashi, Y, Nishikawa, M, Matsui, Y, Fukuhara, Y, Oushiki, D *et al.* (2011). Positive correlation between the generation of reactive oxygen species and activation/reactivation of transgene expression after hydrodynamic injections into mice. *Pharm Res* **28**: 702–711.
49. Gu, SG and Fire, A (2010). Partitioning the C. elegans genome by nucleosome modification, occupancy, and positioning. *Chromosoma* **119**: 73–87.
50. Lee, TI, Johnstone, SE and Young, RA (2006). Chromatin immunoprecipitation and microarray-based analysis of protein location. *Nat Protoc* **1**: 729–748.